

Performance Evaluation of Cooperative NOMA-based Improved Hybrid SWIPT Protocol

Ahmed Al Amin and Soo Young Shin, *Senior Member, IEEE*

Abstract

This study proposes the integration of a cooperative non-orthogonal multiple access (CNOMA) and improved hybrid simultaneous wireless information and power transfer (IHS SWIPT) protocol (termed as CNOMA-IHS) to enhance the spectral efficiency (SE) of a downlink (DL) CNOMA communication system. CNOMA-IHS scheme can enhance the ergodic sum capacity (ESC) and energy efficiency (EE) of DL CNOMA by transferring additional symbols towards the users and energize the relay operation as well without any additional resources (e.g., time slot/frequency/code). The analytical and simulation results indicate that the proposed CNOMA-IHS scheme outperforms other existing SWIPT-based schemes (e.g., CNOMA with hybrid SWIPT, CNOMA with power-splitting SWIPT, wireless-powered CNOMA, CNOMA with time switching SWIPT, and orthogonal multiple access with IHS SWIPT) in terms of the ESC. Moreover, the CNOMA-IHS scheme also enhances EE compared with other conventional TS-SWIPT-based schemes, which is also illustrated by the simulation results. In addition, the proposed CNOMA-IHS scheme with the considered EE optimization technique outperformed the proposed CNOMA-IHS scheme without EE optimization and other existing TS-SWIPT-based schemes in terms of EE.

Index Terms

Cooperative non-orthogonal multiple access, energy efficiency, improved hybrid simultaneous wireless information and power transfer, and sum capacity.

The authors are with the WENS Laboratory, Department of IT Convergence Engineering, Kumoh National Institute of Technology, Gumi 39177, South Korea (e-mail: amin@kumoh.ac.kr; wdragon@kumoh.ac.kr).

Corresponding author: Soo Young Shin (wdragon@kumoh.ac.kr)

I. INTRODUCTION

Non-orthogonal multiple access (NOMA) transmits simultaneous data to multiple users using power or code domain multiplexing technique without additional radio resources [1]. NOMA can provide high spectral efficiency to a considerable number of users [2]. There are two primary types of NOMA techniques: code-domain NOMA and power-domain (PD) NOMA. Code-domain NOMA facilitates user separation at the receiver end by introducing redundancies via coding or spreading. In contrast, PD NOMA can perform successive interference cancellation (SIC) for users having better channel conditions [3-5]. This ensures flexibility in resource allocation as well as improving the performance of NOMA [6]. Hence, PD-NOMA has been considered in this study, and, hereafter, NOMA refers to PD-NOMA in this study.

In downlink (DL) NOMA, superposed signals are transmitted to users simultaneously [1-6]. After receiving the signals, the cell center user (CCU) applies SIC to decode the received signals [4-5]. According to NOMA, the signal power of the cell edge user (CEU) is always higher than that of a CCU. Hence, the signal is directly decoded at the CEU, and the signal of the CCU is considered as noise. NOMA can be applicable for future cellular communication applications [2-10]. One of the research fields related to NOMA is cooperative NOMA (CNOMA) [6-14]. CNOMA can be classified into two major categories. Strong users, such as CCUs, act as relays in the first category, and in the other category, NOMA users are assisted by dedicated relays [6]. In this study, the first category of CNOMA is considered because dedicated relays are not universally available. Moreover, the user-assisted CNOMA enhances the coverage area and data reliability of a wireless communication system considering users with the best channel conditions as relays [6-8]. In the case of the conventional user-assisted CNOMA, CCU has a better channel condition than CEU. Hence, CCU has been considered a relay to enhance the coverage area and data reliability of the CEU in case of user-assisted relaying [9]. The simultaneous wireless information power transfer (SWIPT) protocol can extract energy to perform energy harvesting (EH) from ambient radio frequency signals and also transfer information simultaneously [10-14].

The major challenge of the CCU is to reduce the battery drainage issue while performing the relay operation [10-13]. Such drainage can cause CCU equipment to turn off and terminate the relay operation. Thus, the performance of the network is degrading significantly. To mitigate this problem, a hybrid SWIPT (HS) protocol was proposed and considered for CNOMA (CNOMA-HS) in [11-13]. Moreover, CNOMA-HS scheme can provide more harvested energy

than conventional power splitting (PS) and time switching (TS) based SWIPT protocol because HS protocol is a combination of TS and PS based SWIPT protocol [11–13]. CNOMA with TS and PS-based SWIPT protocol was proposed in recent studies [14–15]. Furthermore, wireless powered CNOMA (WP-CNOMA) was proposed to empower the relay based CNOMA and also enhance the throughput by the proposed technique [14]. In addition, an optimization technique for outage probabilities and ESC in the case of CNOMA with SWIPT protocol was discussed in [15]. But the improvement of user channel capacities and ESC of the CNOMA-HS-SWIPT scheme were not discussed in [11–15]. The main challenges of the CNOMA-HS scheme are the degradation of user channel capacities and ESC because TS and PS SWIPT are combined in the DL CNOMA-HS-SWIPT scheme. Moreover, no suitable technique was proposed for the enhancement of ESC in the case of the DL CNOMA-HS scheme [11-13,15]. Therefore, a suitable HS SWIPT protocol is required which can provide sufficient EH for decode and forward (DF) relay operation and enhance user channel capacities, as well as the ESC of the DL CNOMA without any extra resources (Time/frequency/code) or interference issues [16-17]. Hence, suitable transmission strategies should be integrated with the DL CNOMA-HS scheme so that the channel capacities, along with the ESC, are improved significantly.

Energy efficiency (EE) is another vital factor in case of future wireless communication system in case of wireless information and power transfer [18]. Moreover, SWIPT protocol provides the possibility of improving the EE [19]. Thus, EE improvement is a vital issue in case of CNOMA with SWIPT protocol based scheme [18–19]. But in previous studies, the enhancement of user channel capacities, ESC, and EE of the CNOMA with SWIPT protocol has not been extensively explored. To address this issue, a suitable HS protocol and scheme are required to enhance the ESC and EE using the idle link without any extra resources or interference.

To enhance the user channel capacities, ESC, and EE of a hybrid SWIPT protocol with DL CNOMA, a novel improved hybrid SWIPT (IHS) protocol has been proposed in this study. Moreover, CNOMA is integrated with the IHS protocol which is termed as CNOMA-IHS scheme that enhances the ESC of DL CNOMA cellular networks. This scheme energizes the CCU for DF relay operations and transmits additional symbols to CCU and CEU, which enhance the channel capacity of CCU and CEU using different transmission strategies without consuming any additional resources or introduce any interference issue. This mainly improves the user channel capacities of the proposed scheme compared to the existing schemes. Consequently, the proposed scheme enhances the ESC in comparison with other conventional SWIPT protocol-based schemes

(e.g., CNOMA with HS [11], CNOMA with power-splitting SWIPT (CNOMA-PS) [20], WP-CNOMA[14], CNOMA with time-switching SWIPT (CNOMA-TS) [20], and orthogonal multiple access with IHS (termed as OMA-IHS) schemes). Furthermore, the EE improvement of the proposed scheme is also evaluated and compared to other conventional SWIPT protocol-based schemes as well. As fraction of block time for EH is superior factor than the power splitting ratio in case of hybrid SWIPT protocol [11-13,15]. Hence, fraction of block time for EH based EE optimization technique is considered in this study [18]. In addition, the proposed CNOMA-IHS scheme with the considered EE optimization technique outplayed the proposed CNOMA-IHS scheme without EE optimization technique and other existing SWIPT-based schemes in terms of EE.

The primary contributions of this study are as follows:

- In this study, CNOMA-IHS scheme is proposed considering the CCU as a relay. In addition, CNOMA-IHS scheme reduces the battery drainage issue of the CCU and improves the user capacities, ESC, and EE significantly.
- The ESC of the proposed CNOMA-IHS scheme is analyzed and compared with the existing SWIPT based schemes (e.g., CNOMA-HS[11], CNOMA-PS[20], WP-CNOMA[14], CNOMA-TS[20], and OMA-IHS) as well.
- Moreover, the impact of the different parameters of the SWIPT protocol on the ESC of the proposed CNOMA-IHS scheme are also evaluated and compared with the existing SWIPT-based schemes [11,14,20].
- Using analytical and simulations results, the ESC improvement of the proposed scheme compared with other existing schemes is explicitly evaluated [11,14,20].
- EE of the proposed CNOMA-IHS scheme is evaluated for the proposed scheme and compared with existing SWIPT-based schemes (e.g., CNOMA-HS[11], WP-CNOMA[14], CNOMA-TS[20], and OMA-IHS). Moreover, the impact of fraction of block time for EH on the EE is also evaluated and compared with the existing schemes. Furthermore, the proposed CNOMA-IHS scheme with considered EE optimization is also compared with the proposed scheme without considered EE optimization and other existing SWIPT-based schemes in terms of EE.

The remainder of this paper is organized as follows: Section 2 describes the CNOMA-IHS scheme using the system model. Section 3 evaluates the result analysis. Section 4 concludes the

paper.

II. SYSTEM MODEL AND IHS PROTOCOL

A system model of the DL CNOMA-IHS scheme using a base station (BS) as a source (S) and two users (a CCU called UE_1 and a CEU called UE_2) in a single-cell scenario is considered. The user-assisted energy-constrained relay used to enhance the data reliability and coverage area of the network is denoted as UE_1 [11–13]. Furthermore, UE_1 conducts IHS-based EH to perform DF relaying for UE_2 by the harvested energy. S , UE_1 , and UE_2 are considered as single antenna devices. The system model of the proposed scheme is illustrated in Figure 1. The subscripts S , 1, and 2 correspond to S , UE_1 , and UE_2 , respectively. Here, $d_{S,1}$ and $d_{S,2}$ denote the corresponding normalized distances of UE_1 and UE_2 from S , as depicted in Figure 1. Furthermore, $d_{1,2}$ denotes the normalized distance between UE_1 and UE_2 . The independent Rayleigh fading channel coefficients corresponding to the S -to- UE_1 , S -to- UE_2 , and UE_1 -to- UE_2 links are denoted by $h_{S,1}$, $h_{S,2}$, and $h_{1,2}$, respectively. The channel coefficient $h_{i,j} \sim CN(0, \lambda_{i,j})$ between any two nodes i and j ($i, j \in \{S, UE_1, UE_2\}$ and $i \neq j$) is related to the Rayleigh fading channel, along with the Gaussian random noise with variance σ^2 and zero mean, which are considered in this study [11–13,20]. The path loss exponent of the proposed system model is represented by ν , and the distance in meters is denoted by $d_{i,j}$. Moreover, $\lambda_{S,1} > \lambda_{S,2}$ and $\lambda_{1,2} > \lambda_{S,2}$ because $d_{S,1} < d_{S,2}$ and $d_{1,2} < d_{S,2}$ have been considered in this study. Furthermore, all the Rayleigh fading channel gains are considered complex channel coefficients [11–13,20]. Based on the principle of DL NOMA, p_N and p_F denote the powers allocated from S to UE_1 and UE_2 , respectively, where $p_F > p_N$ because $d_{S,1} < d_{S,2}$, and $p_N + p_F = 1$. In addition, P denotes the total transmission power of S . p_N and p_F can be determined by following equations [11, 21]:

$$p_N = \frac{2^{2R_{th,1}} - 1}{2^{2R_{th,1}+2R_{th,2}} - 1}, \quad (1)$$

$$p_F = 1 - p_N, \quad (2)$$

Where $R_{th,1}$ and $R_{th,2}$ are the targeted data rate of UE_1 and UE_2 , respectively. Moreover, θ ($0 < \theta < 1$) and δ ($0 < \delta < 1$) are the fraction of block time for energy harvesting and power allocation factor for the proposed IHS protocol, respectively [11–13]. A symbol x_1 is transmitted to UE_1 for EH and is simultaneously transmitted to UE_2 for information transmission during phase-1 with P . The NOMA-based superimposed signals are transferred toward the users during

phase-1 as well. So, x_2 and x_3 are transmitted as superimposed signal towards the users during phase-1. Furthermore, a power splitting (PS)-based EH is performed during phase-1 by UE_1 using δ . Moreover, x_2 is decoded using the harvested energy $(1 - \delta)$ by UE_1 . Furthermore, x_3 is directly decoded by UE_2 because $p_F > p_N$ during phase 1.

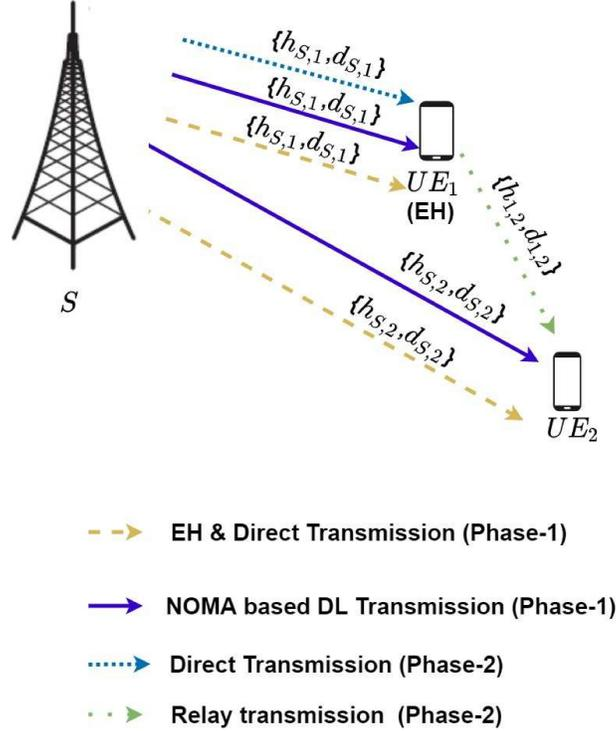


Fig. 1: System model of proposed CNOMA-IHS scheme.

During phase 2, UE_1 performs the DF relaying of x_3 toward UE_2 to enhance data reliability and coverage area of the cellular network. In addition, an additional symbol x_4 by p_N is transmitted to UE_1 from S during second segment of phase 2. The transmission strategies are illustrated in Figure 1.

The proposed protocol of the CNOMA-IHS scheme is depicted in Figure 2, where T denotes the total time duration required for a complete DL transmission. During the first segment of phase 1 (θT duration), x_1 is transmitted to UE_1 and UE_2 , simultaneously. Moreover, x_2 and x_3 are transmitted using the superimposed NOMA signal to UE_1 and UE_2 during the second segment of phase 1 ($((1 - \theta)T/3)$). During first segment of phase 2 ($(1 - \theta)T/3$), UE_1 relays decoded x_3 (\hat{x}_3) to UE_2 to improve data reliability and coverage area of the cellular network. In addition, x_4 is also transmitted from S to UE_1 during second segment of phase 2 ($(1 - \theta)T/3$).

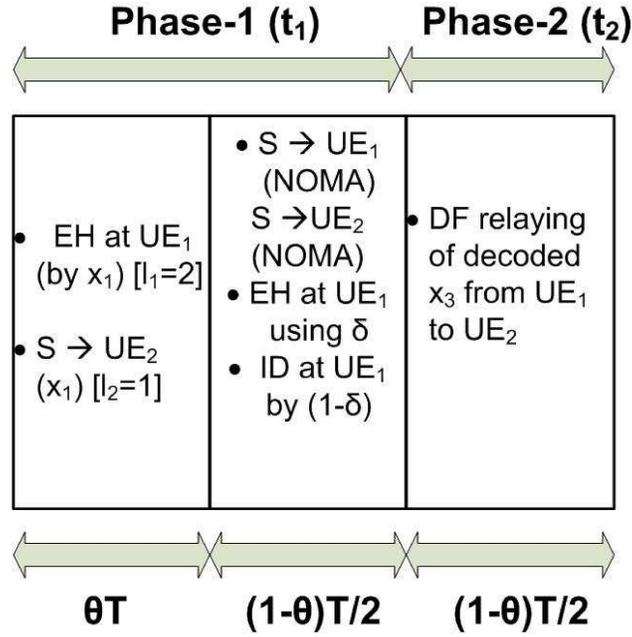


Fig. 2: Proposed protocol of CNOMA-IHS scheme.

The detailed descriptions of the different phases along with the signal-to-interference plus noise ratio (SINR) equations for different symbols are given in the following subsections:

A. Phase-1(t_1)

In the proposed CNOMA-IHS scheme, x_1 is transmitted from S to the users using A_1 signal with transmitted power P . So, A_1 can be expressed as below:

$$A_1 = \sqrt{P}x_1, \quad (3)$$

where x_1 denotes a data symbol for UE_2 . In addition, x_1 is transmitted to UE_1 , which harvests the energy during the first segment of phase 1 (θT). Moreover, A_1 is received by UE_2 and UE_2 decodes x_1 during the first segment of phase 1 (θT). The received signals at UE_1 and UE_2 are expressed by the following equations:

$$y_{S,1}^{t_1} = (\sqrt{P}x_1)h_{S,1} + n_1, \quad (4)$$

$$y_{S,2}^{t_1} = (\sqrt{P}x_1)h_{S,2} + n_2, \quad (5)$$

where $n_1 \sim CN(0, \sigma^2)$ and $n_2 \sim CN(0, \sigma^2)$ are the complex white Gaussian noises at UE_1 and UE_2 , respectively, with variance σ^2 and zero mean. The received SINR for x_1 at UE_2 can be derived as follows:

$$\gamma_{x_1}^{t_1} = \rho |h_{S,2}|^2, \quad (6)$$

where $\rho \triangleq \frac{P}{\sigma^2}$ denotes the transmit signal-to-noise ratio (SNR) and σ^2 denotes the additive white Gaussian noise variance for all received signals described in this study [20]. Following the principles of DL NOMA, during the second segment of phase 1 ($((1-\theta)T/3$)), S transmits the superposition signal (A_2) to UE_1 and UE_2 , as indicated below:

$$A_2 = \sqrt{p_N P} x_2 + \sqrt{p_F P} x_3, \quad (7)$$

where x_2 and x_3 denote the data symbol for UE_1 and UE_2 , respectively [11–12]. UE_1 acquires x_2 using SIC. The imperfect SIC is assumed at UE_1 . Thus, the residual interference due to imperfect SIC is quantified by β ($0 \leq \beta \leq 1$). So, $\beta = 1$ refers to imperfect SIC and $\beta = 0$ refers as perfect SIC [22]. So, the received signals at UE_1 can be expressed by the following equation:

$$y_{S,1}^{t_1} = (\sqrt{p_N(1-\delta)P} x_2 + \beta \sqrt{p_F(1-\delta)P} x_3) h_{S,1} + n_1. \quad (8)$$

The received SINR corresponding to the symbols, x_2 ($\gamma_{x_2}^{t_1}$) and x_3 ($\gamma_{x_3 \rightarrow x_2}^{t_1}$) at UE_1 by SIC can be expressed as follows [11-13,23]:

$$\gamma_{x_2}^{t_1} = \frac{(1-\delta)\rho |h_{S,1}|^2 p_N}{(1-\delta) + 1}. \quad (9)$$

$$\gamma_{x_3 \rightarrow x_2}^{t_1} = \frac{(1-\delta)\rho |h_{S,1}|^2 p_F}{\beta^2(1-\delta)\rho |h_{S,1}|^2 p_N + 1}. \quad (10)$$

Furthermore, IHS-based SWIPT is used at UE_1 [11–13, 23]. According to Figure 2, UE_1 uses the δ proportion of the received power for EH. Moreover, UE_1 uses the fraction $(1-\delta)$ of the received power for information decoding (ID). In addition, the directly received signal at UE_2 from S is expressed as follows:

$$y_{S,2}^{t_1} = (\sqrt{p_N P} x_2 + \sqrt{p_F P} x_3) h_{S,2} + n_2. \quad (11)$$

Furthermore, x_3 is directly decoded by UE_2 using the direct link from S . The received SINR corresponding to x_3 ($\gamma_{x_3}^{t_1}$) at UE_2 can be expressed as follows:

$$\gamma_{x_3}^{t_1} = \frac{\rho |h_{S,2}|^2 p_F}{\rho |h_{S,2}|^2 p_N + 1}. \quad (12)$$

B. Phase-2(t_2)

During phase 2 ($((1 - \theta)T/3$), \hat{x}_3 is transmitted by P_1 from UE_1 to UE_2 by utilizing the harvested energy (Figure 2). It can be assumed that UE_1 can perfectly decode the x_3 symbol during the second segment of phase 1 ($((1 - \theta)T/3$) (Figure 2) [11, 20, 23–24]. The power splitting (PS)-based SWIPT is implemented by UE_1 for EH to relay the decoded \hat{x}_3 from UE_1 to UE_2 . The signal received by the DF relaying from UE_1 to UE_2 can be expressed as follows:

$$y_{1,2}^{t_2} = \sqrt{P_1}\hat{x}_3h_{1,2} + n_2. \quad (13)$$

Thus, the received SINR at UE_2 from UE_1 corresponding to the symbol \hat{x}_3 ($\gamma_{x_3}^{t_2}$) owing to the DF relay can be expressed as follows :

$$\gamma_{x_3}^{t_2} = |h_{1,2}|^2P_1. \quad (14)$$

Thus, the DF relaying from UE_1 to UE_2 is performing by the transmitted power P_1 from UE_1 . P_1 utilizing the harvested energy which can be expressed as follows by [11–13]:

$$P_1 = \frac{E_1}{(1 - \theta)T/3} = \eta\rho|h_{S,1}|^2\left(\frac{3\theta}{1 - \theta} + \delta\right), \quad (15)$$

where $E_1 = \eta\rho|h_{S,1}|^2\theta T + \eta\delta\rho|h_{S,1}|^2(1 - \theta)T/3$ is the harvested energy at UE_1 by IHS protocol [11-13]. Moreover, η represents the energy conversion efficiency that relies on the EH circuit and $0 < \eta < 1$ [11–13,20]. Moreover, S directly transmitted a signal ($A_3 = \sqrt{p_N P}x_4$) from S to UE_1 by $p_N P$ during t_2 . Because, x_4 is only transmitted for UE_1 . So, the signal received at UE_1 during t_2 can be expressed as follows:

$$y_{S,1}^{t_2} = (\sqrt{p_N P}x_4)h_{S,1} + n_1. \quad (16)$$

Thus, the received SINR for x_4 at UE_1 during phase 2 owing to direct transmission can be represented as follows:

$$\gamma_{x_4}^{t_2} = p_N|h_{S,1}|^2\rho. \quad (17)$$

C. Channel Capacities of CNOMA-IHS

By assuming normalized total time duration and total transmit power, the capacity of x_1 can be calculated as follows:

$$C_{x_1} = \theta \log_2(1 + (\gamma_{x_1}^{t_1})). \quad (18)$$

Moreover, the achievable capacities of x_2 and x_3 can be calculated as follows [2,9,11–13,20]:

$$C_{x_2} = \frac{1-\theta}{3}(\log_2(1 + (\gamma_{x_2}^{t_1}))). \quad (19)$$

$$C_{x_3} = \frac{1-\theta}{3}(\log_2(1 + \min(\gamma_{x_3 \rightarrow x_2}^{t_1}, \gamma_{x_3}^{t_1}, \gamma_{x_3}^{t_2}))). \quad (20)$$

In addition, the achievable capacities of x_4 can be calculated as follows [2,9,11–13]:

$$C_{x_4} = \frac{1-\theta}{3} \log_2(1 + (\gamma_{x_4}^{t_2})). \quad (21)$$

Thus, the achievable SC can be calculated using the following equations [2,9,11–13,20]:

$$C_1 = E[C_{x_2}] + E[C_{x_4}]. \quad (22)$$

$$C_2 = E[C_{x_1}] + E[C_{x_3}]. \quad (23)$$

$$C_{sum} = C_1 + C_2, \quad (24)$$

where $E[.]$ represents the mean or expectation operator. Moreover, C_1 , C_2 , and C_{sum} denote the respective channel capacities of UE_1 , UE_2 , and ESC for the proposed CNOMA-IHS scheme.

The analytical ergodic capacity (EC) of UE_1 can be expressed by Theorem 1. The values of the variables are considered identical. Various variables are assumed for information transfer by transmitting various symbols (i.e., x_2 and x_4) from S in different phases for UE_1 , utilizing different power allocations from S in the case of the proposed scheme. The EC in the case of UE_1 for the proposed scheme can be analytically expressed using Theorem 1.

Theorem 1. The EC of UE_1 (C_1^{erg}) in the case of CNOMA-IHS is expressed by the following equation:

$$C_1^{erg} = \frac{1-\theta}{3\ln 2} \left\{ -Ei\left(\frac{-1}{g}\right)e^{\frac{1}{g}} \right\} + \frac{1-\theta}{3\ln 2} \left\{ -Ei\left(\frac{-1}{h}\right)e^{\frac{1}{h}} \right\}, \quad (25)$$

where $g \triangleq (1-\delta)\lambda_{S,1}\rho p_N$ and $h \triangleq \lambda_{S,1}\rho p_N$ due to direct transmission of x_2 by superimposed signal along with PS based EH and direct transmission of x_4 during t_1 and t_2 , respectively. Moreover, $Ei(.)$ denotes the exponential integral function.

Proof. Let $A \triangleq (1-\delta)\rho|h_{S,1}|^2 p_N$ and $B \triangleq \rho|h_{S,1}|^2 p_N$ due to direct transmission of x_2 by superimposed signal along with PS based EH and direct transmission of x_4 during t_1 and t_2 , respectively; the cumulative distributed function (CDF) of A and B can be determined by the following equations[20,25–27]:

$$F_a(A) = 1 - e^{\frac{-a}{(1-\delta)\lambda_{S,1} p_N \rho}}, \text{ and} \quad (26)$$

$$F_b(B) = 1 - e^{\frac{-b}{\lambda_{S,1} \rho p_N}}. \quad (27)$$

The EC of UE_1 can be derived by determining $\int_0^\infty (1+a)f_A(a)da = \frac{1}{\ln 2} \int_0^\infty \frac{1-F_A(a)}{1+a} da$ and $\int_0^\infty (1+b)f_B(b)db = \frac{1}{\ln 2} \int_0^\infty \frac{1-F_B(b)}{1+b} db$. Thus, the EC of UE_1 can be derived as follows :

$$\begin{aligned} C_1^{erg} &= \frac{1-\theta}{3\ln 2} \int_0^\infty \frac{1}{1+a} e^{\frac{-a}{(1-\delta)\lambda_{S,1}\rho p_N}} da + \frac{1-\theta}{3\ln 2} \int_0^\infty \frac{1}{1+b} e^{\frac{-b}{\lambda_{S,1}\rho p_N}}. \\ C_1^{erg} &= \frac{1-\theta}{3\ln 2} \left\{ -Ei\left(\frac{-1}{(1-\delta)\lambda_{S,1}\rho p_N}\right) e^{\frac{1}{(1-\delta)\lambda_{S,1}\rho p_N}} \right\} + \frac{1-\theta}{3\ln 2} \left\{ -Ei\left(\frac{-1}{\lambda_{S,1}\rho p_N}\right) e^{\frac{1}{\lambda_{S,1}\rho p_N}} \right\}, \\ &= \frac{1-\theta}{3\ln 2} \left\{ -Ei\left(\frac{-1}{g}\right) e^{\frac{1}{g}} \right\} + \frac{1-\theta}{3\ln 2} \left\{ -Ei\left(\frac{-1}{h}\right) e^{\frac{1}{h}} \right\}, \end{aligned} \quad (28)$$

where $g \triangleq (1-\delta)\lambda_{S,1}\rho p_N$ and $h \triangleq \lambda_{S,1}\rho p_N$ due to direct transmission of x_2 by superimposed signal along with PS based EH and direct transmission of x_4 during t_1 and t_2 , respectively. Moreover, $Ei(\cdot)$ represents the exponential integral function. \square

The EC of UE_2 for the proposed CNOMA-IHS scheme can be analytically derived using Theorem 2

Theorem 2. The EC of UE_2 (C_2^{erg}) for the CNOMA-IHS scheme is expressed as follows:

$$\begin{aligned} C_2^{erg} &= \frac{1-\theta}{3\ln 2} \left\{ -Ei(-(l+q))e^{(l+q)} \right. \\ &\quad \left. + Ei(-(r+s))e^{(r+s)} \right\} + \frac{\theta}{\ln 2} \left\{ -Ei\left(\frac{-1}{u}\right) e^{\frac{1}{u}} \right\}, \end{aligned} \quad (29)$$

where, $l = \frac{1}{\lambda_{S,1}\rho(1-\delta)}$, $q = \frac{1}{\lambda_{1,2}\rho}$, $r = \frac{1}{\lambda_{S,1}\rho p_N(1-\delta)}$, $s = \frac{1}{\lambda_{1,2}\rho p_N}$, $u = \lambda_{S,2}\rho$, and $Ei(\cdot)$ represents the exponential integral function.

Proof. Let $L \triangleq \frac{\rho|h_{S,1}|^2 p_F(1-\delta)}{\rho|h_{S,1}|^2 p_N(1-\delta)+1}$ by considering the imperfect SIC, $Q \triangleq \frac{\rho|h_{S,2}|^2 p_F}{\rho|h_{S,2}|^2 p_N+1}$, $M \triangleq \min(\gamma_{x_3 \rightarrow x_2}^{t_1}, \gamma_{x_3}^{t_1}, \gamma_{x_3}^{t_2})$, and $V \triangleq \rho|h_{S,2}|^2$. Thus, the CDF of L , Q , M , and V can be written as follows [20,25–27]:

$$F_l(L) = 1 - \frac{\rho\lambda_{S,1}p_F(1-\delta)}{(1-\delta)(\rho\lambda_{S,1}p_F + \rho\lambda_{S,1}p_N)} e^{\frac{-l}{\rho\lambda_{S,1}p_F(1-\delta)}}. \quad (30)$$

$$F_q(Q) = 1 - \frac{\rho\lambda_{S,2}p_F}{\rho\lambda_{S,2}p_F + \rho\lambda_{S,2}p_N} e^{\frac{-q}{\rho\lambda_{S,2}p_F}}. \quad (31)$$

$$F_m(M) = (1 - e^{\frac{-m}{(r+s)}}) - (1 - e^{\frac{-m}{(r+s)}}). \quad (32)$$

$$F_v(V) = 1 - e^{\frac{-v}{\lambda_{S,2}\rho p_N}}. \quad (33)$$

Using $\int_0^\infty (1+m)f_M(m)dm = \frac{1}{\ln 2} \int_0^\infty \frac{1-F_m(M)}{1+m} dm$ and $\int_0^\infty (1+v)f_V(v)dv = \frac{1}{\ln 2} \int_0^\infty \frac{1-F_v(V)}{1+v} dv$, the EC of UE_2 can be written as (29). After the mathematical manipulation, the EC of the UE_2 can be achieved as below [27]:

$$C_2^{erg} = \frac{1-\theta}{3\ln 2} \{-Ei(-(l+q))e^{(l+q)} + Ei(-(r+s))e^{(r+s)}\} + \frac{\theta}{\ln 2} \{-Ei(\frac{-1}{u})e^{\frac{1}{u}}\}. \quad (34)$$

where, $l = \frac{1}{\lambda_{S,1}\rho(1-\delta)}$, $q = \frac{1}{\lambda_{1,2}\rho}$, $r = \frac{1}{\lambda_{S,1}\rho p_N(1-\delta)}$, $s = \frac{1}{\lambda_{1,2}\rho p_N}$, $u = \lambda_{S,2}\rho$, and $Ei(\cdot)$ represents the exponential integral function. \square

By adding (25) and (29), the analytical expression of ESC of the proposed CNOMA-IHS can be derived as follows:

$$C_{sum}^{erg} = C_1^{erg} + C_2^{erg}. \quad (35)$$

D. Energy Efficiency of CNOMA-IHS

The evaluation of EE and the optimization technique of EE for the proposed CNOMA-IHS scheme is describe in this subsection. UE_1 uses the energy harvested by the proposed CNOMA-IHS scheme to conduct a relay operation. The relay of \hat{x}_3 from UE_1 to UE_2 is conducted during phase 2 of the proposed IHS protocol using P_1 . Thus, EE is the ratio of the ESC (C_{sum}) to the total transmit power for direct transmission ($2P$ and p_N) and transmit power of UE_1 for DF-based relay operation (P_1) [28]. Therefore, the EE corresponding to the proposed CNOMA-IHS scheme can be derived using the following equation:

$$EE = \frac{C_{sum}}{2P + P_1 + p_N}. \quad (36)$$

As θ is the dominating factor than δ in case of HS SWIPT protocol [11–13]. Hence θ based EE optimization technique is considered for the proposed CNOMA-IHS scheme [18]. Thus, the optimal θ (θ^*) can be derived to achieve EE maximization by below equation:

$$\theta^* = 1 - \frac{E_1}{\eta|h_{S,1}|^2(2P + P_1 + p_N)}. \quad (37)$$

E. OMA-IHS

As benchmark, OMA-IHS scheme is considered and compared with the proposed CNOMA-IHS scheme for fair comparisons. In the case of OMA, time division multiple access has been

considered in this study. In this scenario, S directly delivers different information signals to UE_1 and UE_2 separately using various independent time slots. Furthermore, one additional time slot is required to perform TS-based EH at UE_1 . Moreover, an additional time slot is required to perform the DF relay of \hat{x}_3 from UE_1 to UE_2 . Various independent time slots are allocated for UE_1 and UE_2 related to various symbols for information transfer (e.g., x_1 , x_2 , x_3 , and x_4), EH (e.g., EH at UE_1) and for DF relaying of \hat{x}_3 are denoted by t_1 , t_2 , t_3 , t_4 , t_5 , and t_6 , respectively, because the IHS protocol is a combination of TS and PS-based SWIPT. Total six time slots are used in case of OMA-IHS scheme. Among them, four time slots are used for information transfer from S to the users and one time slot is using for TS-based EH and another for DF relaying. At first, x_1 is transmitted to UE_1 during t_1 for the TS-based EH. Then, x_1 is transmitted to UE_2 during t_2 for information transfer. In addition, x_2 is transmitted from S to UE_1 by t_3 for information transfer. In the case of PS-based SWIPT, UE_1 uses a fraction (δ) of the received power for EH. Furthermore, the rest of the fraction ($1 - \delta$) of the received power is used for ID during time slot t_3 [17, 20]. Subsequently, x_3 is transmitted from S to UE_2 by t_4 for information transfer. Moreover, \hat{x}_3 relays from UE_1 to UE_2 during t_5 using the power (P_1) which utilizing the harvested energy. Afterwards, x_4 is directly transmitted to UE_1 from S during t_6 for information transfer as well. All these transmissions are performed by the total transmit power of P from S . In addition, $t_1 = t_2 = t_3 = t_4 = t_5 = t_6 = \frac{1}{6}$ are considered in this study for the OMA-IHS scheme to complete all the EH, information transfer, and relaying. Thus, the capacity of x_1 at UE_2 in the case of OMA-IHS can be expressed as follows [2,20,25–26]:

$$C_{x_1}^{OMA} = \frac{1}{6}(\log_2(1 + (\gamma_{x_1}^{OMA}))). \quad (38)$$

In addition, the achievable capacities of x_2 and x_3 corresponding to the OMA-IHS scheme can be calculated as follows [2,20,24,26]:

$$C_{x_2}^{OMA} = \frac{1}{6}(\log_2(1 + (\gamma_{x_2}^{OMA}))), \quad (39)$$

$$C_{x_3}^{OMA} = \frac{1}{6}(\log_2(1 + \min(\gamma_{x_3}^{OMA}, \gamma_{\hat{x}_3}^{OMA}))), \text{ and} \quad (40)$$

$$C_{x_4}^{OMA} = \frac{1}{6}(\log_2(1 + (\gamma_{x_4}^{OMA}))), \quad (41)$$

where $\gamma_{x_1}^{OMA} = \rho|h_{S,2}|^2P$, $\gamma_{x_2}^{OMA} = (1 - \delta)\rho|h_{S,1}|^2P$, $\gamma_{x_3}^{OMA} = (1 - \delta)\rho|h_{S,1}|^2P$, $\gamma_{x_4}^{OMA} = \rho|h_{S,1}|^2P$, $\gamma_{\hat{x}_3}^{OMA} = \rho|h_{1,2}|^2P_1^{OMA}$, $\gamma_{x_4}^{OMA} = \rho|h_{1,2}|^2P$, and $P_1^{OMA} = \eta\rho|h_{S,1}|^2(\frac{6\theta}{1-\theta} + \delta)$. Thus, the ESC of the OMA-IHS scheme can be expressed as follows [2,20,25–26]:

$$C_1^{OMA} = E[C_{x_2}^{OMA}] + E[C_{x_4}^{OMA}]. \quad (42)$$

$$C_2^{OMA} = E[C_{x_1}^{OMA}] + E[C_{x_3}^{OMA}]. \quad (43)$$

$$C_{sum}^{OMA} = C_1^{OMA} + C_2^{OMA}. \quad (44)$$

Here, $E[.]$ denotes the expectation operator. C_1^{OMA} , C_2^{OMA} , and C_{sum}^{OMA} denote the respective channel capacities of UE_1 , UE_2 , and ESC in case of the OMA-IHS scheme. Moreover, the associated EE for the OMA-IHS can be derived using the following equation [13,15,28]:

$$EE_{OMA} = \frac{C_{sum}^{OMA}}{5P + P_1^{OMA}}. \quad (45)$$

Therefore, the aforementioned equation demonstrates that EE is related to C_{sum}^{OMA} , P , and P_1^{OMA} .

III. RESULT ANALYSIS

The results of the ESC of the proposed CNOMA-IHS scheme and the compared existing schemes (e.g., CNOMA-HS[11], WP-CNOMA[14], CNOMA-PS[20], CNOMA-TS[20], and OMA-IHS) are evaluated in this section. All the simulation result evaluations were performed using MATLAB. Moreover, the impacts of θ , δ , and η are examined for the proposed CNOMA-IHS scheme and other compared schemes. In addition, the impact of the transmit SNR (ρ) and the distance between S and UE_1 ($d_{S,1}$) on ESC in case of the proposed scheme and other compared schemes have been evaluated. A comparative analysis in terms of EE corresponding to the proposed CNOMA-IHS scheme and other compared schemes has been presented. The EE of the proposed CNOMA-IHS scheme with the EE optimization technique and without EE optimization technique are compared with other existing schemes is also presented in this section. The impact of θ on the EE in case of the proposed CNOMA-IHS scheme and other compared schemes have been also evaluated in this section. It should be noted that similar simulation parameters have been applied to the proposed and other compared schemes.

A. Ergodic Sum Capacity (ESC)

Figure 3 illustrates that the proposed scheme exhibits a higher capacity than the conventional schemes for different transmit SNRs (ρ). The parameters, $T = 1$, $d_{S,1} = 0.6$, $d_{S,2} = 1$, $\eta = 1$, $\delta = \theta = 0.4$, $R_{th,1} = R_{th,2} = 0.3$, $\beta = 1$, $v = 2$, and $d_{1,2} = d_{S,2} - d_{S,1}$, are considered for the MATLAB simulation. Moreover, for each value of ρ , the ESC of the proposed CNOMA-IHS scheme is significantly higher than those of the other schemes. This is because the additional symbols (x_1 and x_4) are transmitted to UE_2 and UE_1 , respectively, using the CNOMA-IHS

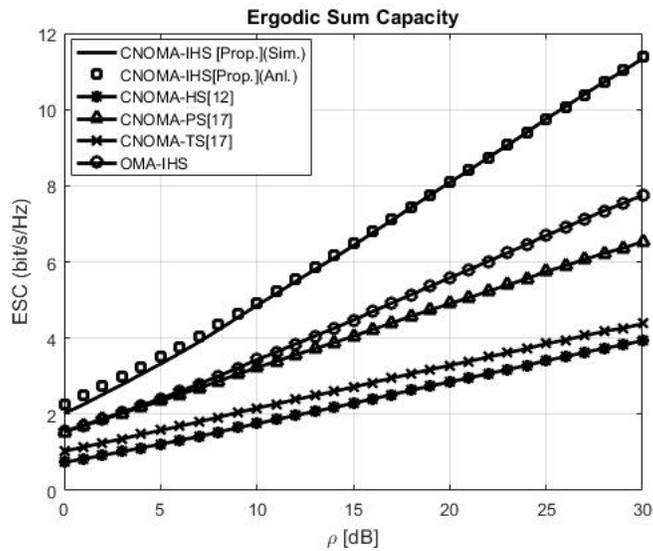


Fig. 3: Comparisons of ESC versus ρ .

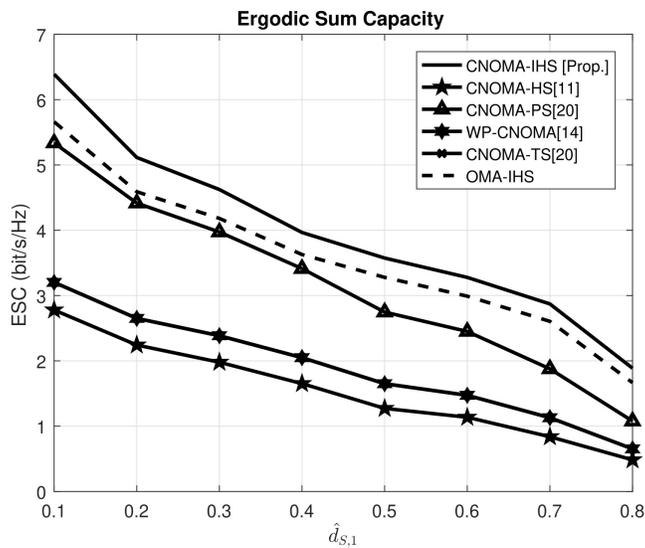
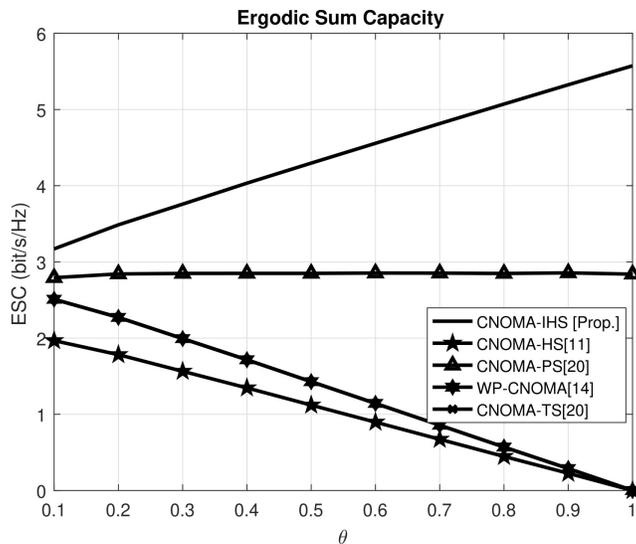
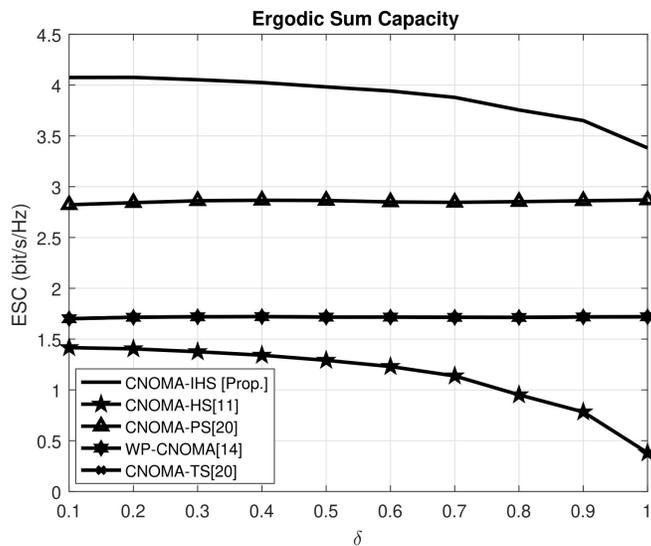


Fig. 4: Comparisons of ESC versus $d_{S,1}$.

scheme without consuming any additional resource. Hence, the user channel capacities and ESC improvement is achieved for the proposed scheme. Thus, the proposed scheme exhibits higher ESC than the other compared schemes. Moreover, the analytical results validate the simulation results of ESC for the proposed CNOMA-IHS scheme which depicted in Figure 3.

Figure 4 illustrates that owing to an increase in $d_{S,1}$, the ESC corresponding to the proposed

Fig. 5: Impact of θ on the ESC.Fig. 6: Impact of δ on the ESC.

scheme is higher than those corresponding to other compared schemes. The parameters, $T = 1$, $d_{S,2} = 1$, $\eta = 1$, $\delta = \theta = 0.4$, $\rho = 15dB$, $R_{th,1} = R_{th,2} = 0.3$, $\beta = 1$, $v = 2$, and $d_{1,2} = d_{S,2} - d_{S,1}$, are considered for the simulation. The position of the relaying node (UE_1) varies depending on the variations of $d_{S,1}$. But x_1 and x_4 are transmitted towards UE_1 and UE_2 during phase-1 and phase-2, respectively. Thus, the achieved ESC is significantly higher than the other compared

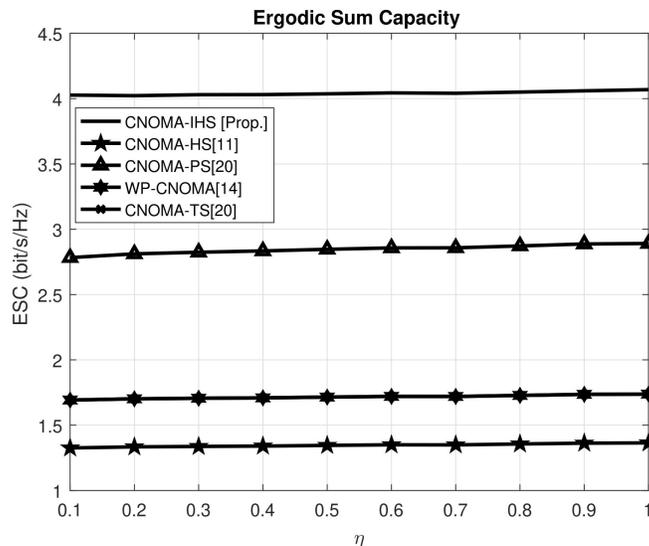


Fig. 7: Impact of η on the ESC.

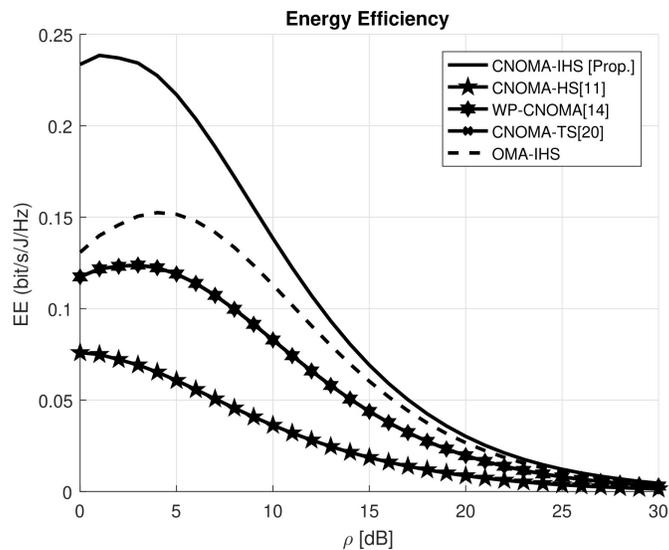


Fig. 8: Comparisons of EE with respect to ρ .

schemes. Furthermore, in the case of the proposed scheme, the amount of energy harvested is higher than those of the other schemes, as CNOMA-IHS comprises PS- and TS-based SWIPT protocols. Thus, the harvested energy is sufficient for the relay operation by UE_1 in the case of higher values of $d_{S,1}$ corresponding to the proposed CNOMA-IHS scheme.

The comparative analysis depicted in Figure 5 indicates that increasing θ influences the ESC

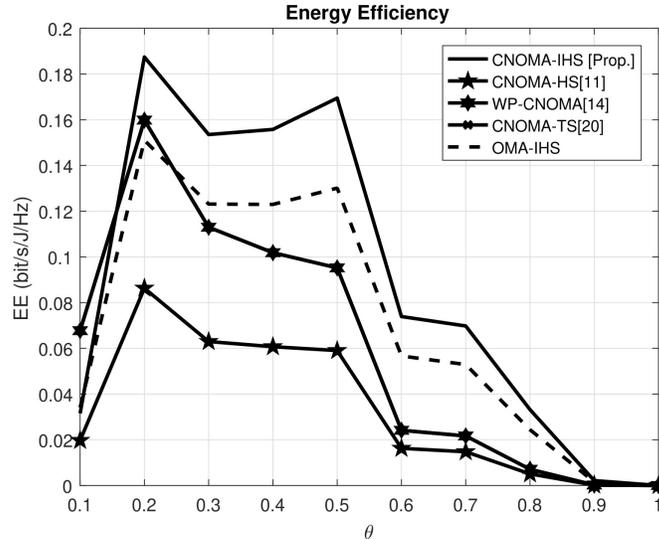


Fig. 9: Comparisons of EE with respect to θ .

of the proposed CNOMA-IHS scheme. The parameters, $T = 1$, $d_{S,1} = 0.6$, $d_{S,2} = 1$, $\rho = 15dB$, $\delta = 0.4$, $\eta = 1$, $R_{th,1} = R_{th,2} = 0.3$, $\beta = 1$, $v = 2$, and $d_{1,2} = d_{S,2} - d_{S,1}$, are considered for the MATLAB simulation. For increasing values of θ , ESC decreases significantly in the case of conventional TS-SWIPT protocol based schemes (CNOMA-HS [11], WP-CNOMA [14], and CNOMA-TS [20]) but ESC increases significantly in the case of the proposed CNOMA-IHS scheme. Because of the higher value of θ can enhance the harvested energy at UE_1 for relaying. Hence, only θT segment of phase-1 is directly involved to perform TS-based EH at UE_1 in the case of conventional TS-SWIPT protocol based schemes (CNOMA-HS[12] (HS protocol is the combination of TS and PS based SWIPT), WP-CNOMA[22], and CNOMA-TS[20]). Hence, the remaining time segments are not sufficient which are used for NOMA-based direct transmission, and DF relaying [11–13,20,23]. Therefore, higher values of θ degrade the user capacities of the conventional TS-based SWIPT schemes. Hence, the ESC of the CNOMA-HS [12], WP-CNOMA [14], and CNOMA-TS [20] schemes, is degraded owing to the increasing values of θ . In contrast, x_1 is transmitted to UE_2 during the first segment of phase-1 (θT) along with the TS-based EH at UE_1 , which enhances the capacity of UE_2 as well as ESC of the proposed CNOMA-IHS scheme. Though other time segments of the protocol for the proposed CNOMA-IHS scheme are not sufficient to perform direct transmission and DF relaying. Thus, the proposed CNOMA-IHS scheme provides higher ESC than other compared TS-SWIPT based CNOMA schemes owing

to increasing values of θ .

The comparative analysis illustrated in Figure 6 indicates that δ influences the ESC of the proposed CNOMA-IHS scheme. The parameters, $T = 1$, $d_{S,1} = 0.6$, $d_{S,2} = 1$, $\rho = 15dB$, $\theta = 0.4$, $\eta = 1$, $R_{th,1} = R_{th,2} = 0.3$, $\beta = 1$, $v = 2$, and $d_{1,2} = d_{S,2} - d_{S,1}$, are considered for the MATLAB simulation. The ESC is decreasing in the case of the proposed and PS-based schemes (CNOMA-IHS, CNOMA-HS[12], and CNOMA-PS[20]) for increasing values of δ . Due to the higher value of δ , the harvested energy at UE_1 is increase but the ID cannot perform successfully because $(1 - \delta)$ amount of energy is used for ID at UE_1 which is degraded due to the higher value of δ . Hence, the relaying cannot perform effectively by UE_1 since the signal decoding cannot perform successfully by less amount of energy due to the higher value of δ . Furthermore, in the case of the proposed CNOMA-IHS scheme, additional symbols (x_1 and x_4) are transmitted to UE_2 and UE_1 without consuming any additional resources or interference. Hence, the higher individual user channel capacities and higher ESC are also achieved for the proposed scheme due to different values of δ .

The comparative analysis depicted in Figure 7 indicates the impact of η on the ESC of the proposed scheme and the other conventional schemes. The parameters, $T = 1$, $d_{S,1} = 0.6$, $d_{S,2} = 1$, $\rho = 15dB$, $\delta = \theta = 0.4$, $R_{th,1} = R_{th,2} = 0.3$, $\beta = 1$, $v = 2$, and $d_{1,2} = d_{S,2} - d_{S,1}$, are considered for the MATLAB simulation. Figure 7 illustrates that η does not have much influence on the ESC in the case of the proposed scheme and other compared schemes. However, CNOMA-IHS transmits the additional symbols (x_1 and x_4) to the users utilizing different phases without consuming any additional resources or any interference issue. Hence, the user channel capacities, as well as ESC, corresponding to the proposed CNOMA-IHS scheme are significantly higher compared with the other schemes for different values of η .

B. Energy Efficiency (EE)

The EE comparisons between the proposed CNOMA-IHS scheme and the other compared schemes are depicted in Figure 8 with and without the EE optimization technique. The parameters, $T = 1$, $d_{S,1} = 0.5$, $d_{S,2} = 1$, $\eta = 1$, $\delta = \theta = 0.4$, $\rho = 15dB$, $R_{th,1} = R_{th,2} = 0.3$, $\beta = 1$, $v = 2$, and $d_{1,2} = d_{S,2} - d_{S,1}$, are considered for the MATLAB simulation. The CNOMA-IHS exhibits higher EE than other TS-based compared schemes (e.g., CNOMA-HS[11], WP-CNOMA[14], CNOMA-TS[20], and OMA-IHS). This phenomenon occurs because additional symbols (x_1 and x_4) are transmitted to the users by the proposed CNOMA-IHS scheme to

enhance the ESC of the proposed compared scheme. This leads to the use of additional power by the proposed scheme but significantly higher ESC is also achieved by the proposed CNOMA-IHS scheme. Thus, the proposed scheme outperforms the other schemes in case of EE without EE optimization. In addition, due to the optimized value of θ (θ^*), significant EE gain can be achieved in the case of the proposed CNOMA-IHS scheme with EE optimization compared to the proposed scheme without EE optimization.

The comparative analysis depicted in Figure 9 indicates that increasing θ influences the EE of the proposed CNOMA-IHS scheme. The parameters, $T = 1$, $d_{S,1} = 0.6$, $d_{S,2} = 1$, $\rho = 15dB$, $\delta = 0.4$, $\eta = 1$, $R_{th,1} = R_{th,2} = 0.3$, $\beta = 1$, $v = 2$, and $d_{1,2} = d_{S,2} - d_{S,1}$, are considered for the MATLAB simulation. For increasing values of θ , EE decreases significantly in the case of the proposed CNOMA-IHS scheme and conventional TS-SWIPT protocol-based schemes (CNOMA-HS [11], WP-CNOMA [14], and CNOMA-TS [20]) schemes. Because the higher value of θ can enhance the harvested energy at UE_1 for relaying. Hence, only θT segment of phase-1 is directly involved to perform TS-based EH at UE_1 in the case of the proposed CNOMA-IHS scheme and other conventional TS-SWIPT protocol based schemes as well (CNOMA-HS[12] (HS protocol is the combination of TS and PS based SWIPT), WP-CNOMA[22], and CNOMA-TS[20]). For increasing values of θ , EE decreases significantly in the case of all SWIPT protocol-based schemes (CNOMA-IHS [Prop.], CNOMA-HS [11], WP-CNOMA [14], and CNOMA-TS [20]). Because a higher value of θ can enhance the harvested energy at UE_1 for relaying. So, higher transmitted power is utilized a higher amount of harvested energy for the same amount of ESC. Moreover, in the case of the proposed CNOMA-IHS scheme the transmitted power is higher cause x_4 is transmitted during phase-2 with p_N compared to conventional CNOMA-HS scheme. But the proposed CNOMA-IHS scheme provides significantly higher EE than other conventional schemes because higher ESC is achieved in case of the CNOMA-IHS scheme compared to other existing schemes.

IV. CONCLUSION

In this study, a CNOMA-IHS scheme was proposed, and its performance was evaluated in terms of ESC and EE. The CCU was used as a DF relay for the CEU in the proposed scheme. The ESC of the proposed CNOMA-IHS scheme was evaluated and compared with CNOMA and existing SWIPT protocol-based schemes (e.g., CNOMA-HS[11], CNOMA-PS[20], WP-CNOMA[14], and CNOMA-TS[20] and the OMA-IHS scheme). The advantages of the proposed

CNOMA-IHS scheme over other compared schemes were demonstrated based on the evaluation of the analytical and simulation results. To evaluate the system performance in terms of ESC, the impact of different parameters (e.g., δ , θ , η , ρ , and $d_{S,1}$) on the ESC was investigated. The proposed CNOMA-IHS scheme was superior to the conventional SWIPT based schemes in terms of ESC, as evidenced by the simulation and analytical results. Furthermore, the EE of the proposed CNOMA-IHS scheme was higher than that of the conventional TS-SWIPT based schemes (e.g., CNOMA-HS[11], WP-CNOMA [14], CNOMA-TS[20], and OMA-IHS). Moreover, the impact of θ on EE in the case of the proposed scheme and other compared schemes are also illustrated by simulation results. In addition, due to the considered EE optimization technique with the CNOMA-IHS scheme provide significantly higher EE than the proposed CNOMA-IHS without EE optimization technique and existing TS-SWIPT based schemes. This study can be extended by integrating the multi-antenna-based BS and transmit antenna selection technique with the proposed CNOMA-IHS scheme.

ACKNOWLEDGMENT

This work was supported by the National Research Foundation of Korea (NRF) funded by the Korean government (MSIT) under grant No. 2019R1A2C1089542.

REFERENCES

- [1] L. Dai, B. Wang, Z. Ding, Z. Wang, S. Chen and L. Hanzo, "A Survey of Non-Orthogonal Multiple Access for 5G," in *IEEE Communications Surveys & Tutorials*, vol. 20, no. 3, pp. 2294-2323, thirdquarter 2018.
- [2] M. B. Shahab, M. F. Kader and S. Y. Shin, "A Virtual User Pairing Scheme to Optimally Utilize the Spectrum of Unpaired Users in Non-orthogonal Multiple Access," in *IEEE Signal Processing Letters*, vol. 23, no. 12, pp. 1766-1770, Dec. 2016.
- [3] Wan, M. Wen, X. Cheng, S. Mumtaz and M. Guizani, "A Promising Non-Orthogonal Multiple Access Based Networking Architecture: Motivation, Conception, and Evolution," in *IEEE Wireless Communications*, vol. 26, no. 5, pp. 152-159, October 2019.
- [4] A. A. Amin and S. Y. Shin, "Channel Capacity Analysis of Non-Orthogonal Multiple Access With OAM-MIMO System," in *IEEE Wireless Communications Letters*, vol. 9, no. 9, pp. 1481-1485, Sept. 2020.
- [5] G. Song and X. Wang, "Comparison of Interference Cancellation Schemes for Non-Orthogonal Multiple Access System," 2016 IEEE 83rd Vehicular Technology Conference (VTC Spring), Nanjing, 2016, pp. 1-5.
- [6] S. M. R. Islam, N. Avazov, O. A. Dobre and K. Kwak, "Power-Domain Non-Orthogonal Multiple Access (NOMA) in 5G Systems: Potentials and Challenges," in *IEEE Communications Surveys & Tutorials*, vol. 19, no. 2, pp. 721-742, Secondquarter 2017.
- [7] Z. Ding, X. Lei, G. K. Karagiannidis, R. Schober, J. Yuan and V. K. Bhargava, "A Survey on Non-Orthogonal Multiple Access for 5G Networks: Research Challenges and Future Trends," in *IEEE Journal on Selected Areas in Communications*, vol. 35, no. 10, pp. 2181-2195, Oct. 2017.

- [8] J. N. Laneman, D. N. C. Tse and G. W. Wornell, "Cooperative diversity in wireless networks: Efficient protocols and outage behavior," in *IEEE Transactions on Information Theory*, vol. 50, no. 12, pp. 3062-3080, Dec. 2004.
- [9] M. F. Kader, M. B. Uddin, S. R. Islam, and S. Y. Shin, "Capacity and outage analysis of a dual-hop decode-and-forward relay-aided NOMA scheme," *Digital Signal Processing*, vol. 88, pp. 138–148, 2019.
- [10] R. Jiao, L. Dai, J. Zhang, R. MacKenzie and M. Hao, "On the Performance of NOMA-Based Cooperative Relaying Systems Over Rician Fading Channels," in *IEEE Transactions on Vehicular Technology*, vol. 66, no. 12, pp. 11409-11413, Dec. 2017.
- [11] T. N. Do, D. B. da Costa, T. Q. Duong and B. An, "Improving the Performance of Cell-Edge Users in MISO-NOMA Systems Using TAS and SWIPT-Based Cooperative Transmissions," in *IEEE Transactions on Green Communications and Networking*, vol. 2, no. 1, pp. 49-62, March 2018.
- [12] N. T. Do, D. Benevides da Costa, T. Q. Duong and B. An, "Transmit antenna selection schemes for MISO-NOMA cooperative downlink transmissions with hybrid SWIPT protocol," *2017 IEEE International Conference on Communications (ICC)*, Paris, 2017, pp. 1-6.
- [13] A. A. Amin and S. Y. Shin, "Investigate the Dominating Factor of Hybrid SWIPT Protocol by Performance Analysis of the Far User of Hybrid SWIPT based CNOMA Downlink Transmission," *2019 International Conference on Electrical, Computer and Communication Engineering (ECCE)*, Cox'sBazar, Bangladesh, 2019, pp. 1-6.
- [14] Y. Zhang, S. Feng and W. Tang, "Performance Analysis and Optimization for Power Beacon-Assisted Wireless Powered Cooperative NOMA Systems," in *IEEE Access*, vol. 8, pp. 198436-198450, 2020, doi: 10.1109/ACCESS.2020.3034917.
- [15] Do DT, Le CB. Application of NOMA in Wireless System with Wireless Power Transfer Scheme: Outage and Ergodic Capacity Performance Analysis. *Sensors (Basel)*. 2018 Oct 17;18(10):3501. doi: 10.3390/s18103501. PMID: 30336586; PMCID: PMC6210380.
- [16] H. Liu, Z. Ding, K. J. Kim, K. S. Kwak and H. V. Poor, "Decode-and-Forward Relaying for Cooperative NOMA Systems With Direct Links," in *IEEE Transactions on Wireless Communications*, vol. 17, no. 12, pp. 8077-8093, Dec. 2018.
- [17] Z. Yang, Z. Ding, Y. Wu and P. Fan, "Novel relay selection strategies for cooperative NOMA", *IEEE Trans. Veh. Technol.*, vol. 66, no. 11, pp. 10114-10123, Nov. 2017.
- [18] J. Tang et al., "Energy Efficiency Optimization for NOMA With SWIPT", in *IEEE Journal of Selected Topics in Signal Processing*, vol. 13, no. 3, pp. 452-466, June 2019, doi: 10.1109/JSTSP.2019.2898114.
- [19] X. Lu, P. Wang, D. Niyato, D. I. Kim and Z. Han, "Wireless Networks With RF Energy Harvesting: A Contemporary Survey," in *IEEE Communications Surveys and Tutorials*, vol. 17, no. 2, pp. 757-789, Second quarter 2015, doi: 10.1109/COMST.2014.2368999.
- [20] M. F. Kader, M. B. Uddin, A. Islam, and S. Y. Shin, "Cooperative non-orthogonal multiple access with SWIPT over Nakagami- m fading channels," *Transactions on Emerging Telecommunications Technologies*, vol. 30, no. 5, 2019.
- [21] Z. Yang, Z. Ding, P. Fan and N. Al-Dhahir, "The Impact of Power Allocation on Cooperative Non-orthogonal Multiple Access Networks With SWIPT," in *IEEE Transactions on Wireless Communications*, vol. 16, no. 7, pp. 4332-4343, July 2017, doi: 10.1109/TWC.2017.2697380.
- [22] I. Abu Mahady, E. Bedeer, S. Ikki and H. Yanikomeroglu, "Sum-Rate Maximization of NOMA Systems Under Imperfect Successive Interference Cancellation," in *IEEE Communications Letters*, vol. 23, no. 3, pp. 474-477, March 2019, doi: 10.1109/LCOMM.2019.2893195.
- [23] G. Li and D. Mishra, "Rate-Constrained Energy Minimization in Hybrid SWIPT for Relay-Assisted NOMA Networks," *2020 IEEE International Conference on Communications Workshops (ICC Workshops)*, Dublin, Ireland, 2020, pp. 1-6, doi: 10.1109/ICCWorkshops49005.2020.9145250.

- [24] Z. Ding, M. Peng and H. V. Poor, "Cooperative Non-Orthogonal Multiple Access in 5G Systems," in *IEEE Communications Letters*, vol. 19, no. 8, pp. 1462-1465, Aug. 2015.
- [25] M. F. Kader and S. Y. Shin, "Coordinated Direct and Relay Transmission Using Uplink NOMA," in *IEEE Wireless Communications Letters*, vol. 7, no. 3, pp. 400-403, June 2018.
- [26] M. F. Kader, S. Y. Shin and V. C. M. Leung, "Full-Duplex Non-Orthogonal Multiple Access in Cooperative Relay Sharing for 5G Systems," in *IEEE Transactions on Vehicular Technology*, vol. 67, no. 7, pp. 5831-5840, July 2018, doi: 10.1109/TVT.2018.2799939.
- [27] M. B. Shahab and S. Y. Shin, "A Time Sharing Based Approach to Accommodate Similar Gain Users in NOMA for 5G Networks," 2017 IEEE 42nd Conference on Local Computer Networks Workshops (LCN Workshops), Singapore, 2017, pp. 142-147, doi: 10.1109/LCN.Workshops.2017.76.
- [28] Y. Huang, M. Liu and Y. Liu, "Energy-Efficient SWIPT in IoT Distributed Antenna Systems," in *IEEE Internet of Things Journal*, vol. 5, no. 4, pp. 2646-2656, Aug. 2018.